

Supporting Information

Tumor oxygen microenvironment-tailored electron transfer-type photosensitizers for precise cancer therapy

Yiting Yang,^a Yafu Wang,^a Yang Liu,^a Kui Wang,^a Ge Wang,^b Yonggang Yang,^a Won jun Jang,^d Tony D. James,^{a,c} Juyoung Yoon ^{*d} and Hua Zhang ^{*a}

^a Key Laboratory of Green Chemical Media and Reactions, Ministry of Education; Collaborative Innovation Centre of Henan Province for Green Manufacturing of Fine Chemicals; Organic Functional Molecules and Drug Innovation Key Laboratory of Henan Province; School of Chemistry and Chemical Engineering, Henan Normal University, Xinxiang, Henan 453007, P. R. China

^b College of Basic Medicine, Xinxiang Medical University, Xinxiang, Henan 453007, P. R. China

^c Department of Chemistry, University of Bath, Bath, BA2 7AY, UK

^d Department of Chemistry and Nanoscience, Ewha Womans University, Seoul 03760, Korea

Corresponding author E-mail: jyoony@ewha.ac.kr, zhh1106@htu.edu.cn

Table of contents

1. Experimental Procedures.....	S2
2. Synthesis of NO ₂ -TPA, NH ₂ -TPA and H-TPA.....	S7
3. Properties of photosensitizers.....	S9
4. Establishing an anoxic model in solution.....	S16
5. Transient absorption spectra and electron receptor quenching evaluation.....	S17
6. TCNQ induces electron transfer.....	S18
7. Excited S1 state REDOX potential.....	S19
8. Lipid droplet colocalization experiments.....	S20
9. MTT Cell survival assay.....	S21
10. Mitochondrial membrane potential laser confocal imaging.....	S23
11. High throughput cell flow cytometry.....	S24
12. Oxygen content in tumor tissue.....	S25
13. Fluorescence imaging of mouse tumors.....	S26
14. NMR spectra and Q-TOF-MS.....	S27

1. Experimental Procedures

1.1 Materials

This study used reagents and solvents of A.R. grade. Column chromatography with silica gel (200-300 mesh), was used to purify all products. All experiments used double-purified water prepared using a Milli-Q system. For spectroscopic analysis and cell studies, stock solutions of **NO₂-TPA**, **NH₂-TPA** and **H-TPA** were used. An Avance 400 or 600 MHz spectrometer (Bruker Co., Switzerland) was used to obtain the NMR spectra. The molecular masses were determined using high resolution mass spectrometry (Water SYNAPT G2-Si, England). The absorption and fluorescence spectra were measured in vitro using a Fluormax-4 spectrophotometer (HORIBA-PLUS-C) and the GBC-Cintra 2020 spectrophotometer. EPR evaluation was conducted using a Bruker EMXnano. An Olympus FV1200 spectral confocal multiphoton microscope was used to capture images of the cells. Cell phototoxicity was determined using the cell phototoxicity irradiator (Puri Material Technology Co., LTD.). For feeding the mice, an independent ventilated cage box system (IVC, Xinhua Medical Device Co., LTD) was used. To assess the impact of photodynamic treatment on living tumors, a homogeneous xenon light source system (CEL-PE300L-3A, Beijing Zhongjiao Jinyuan Technology Co., LTD.) was employed.

1.2 Spectroscopic response of NO₂-TPA to nitro-reductase in solution

NO₂-TPA (10 μM) was dissolved in 3.0 mL double purified water. The fluorescence spectra were measured with a Fluoromax-4 spectrophotometer from HORIBA-PLUS-C. The prepared nitroreductase (NTR) and - nicotinamide adenine dinucleotide (NAD⁺) test solution was then added in accordance with a predetermined concentration gradient. The differences in the fluorescence spectra of dye molecules before and after the addition of NTR and NAD⁺ test solution was used to assess how **NO₂-TPA** responded to these compounds. The parameters of the fluorescence spectrometer used in this experiment were identical before and after the addition of the response material, and the experimental results were obtained by averaging the results of three parallel experiments (n=3).

1.3 Establishing mild, moderate and severe hypoxia environments

In the presence of sufficient oxygen, the fluorescence of Tris (4,7-diphenyl-1,10-phenanthroline) ruthenium (II) dichloride ([Ru(dpp)₃]Cl₂, luminescent oxygen sensor) is weak, but it can be enhanced by hypoxia. An oxygen indicating probe was used to detect the fluorescence signal after injecting gas into the solution with varying oxygen

contents to mimic the solution's varying oxygen content. Different oxygen content and fluorescence intensity were used to plot the relationship between the oxygen content and fluorescence intensity.

1.4 ROS production in the presence and absence of oxygen in solution

The compound 2',7'-dichlorodihydrofluorescein (DCFH) was used as an indicator of ROS in solution. Non-fluorescent substance DCFH can be oxidized by reactive oxygen species to produce a strongly fluorescent substance DCF, which emits fluorescence at 523 nm. **NO₂-TPA** (10 μ M) and DCFH (40 μ M) were dissolved in 3 mL double purified water. The mixture was placed in a quartz cuvette and illuminated by a xenon lamp of 5 mW cm⁻². The change of fluorescence intensity at 523 nm was recorded using a fluorescence spectrophotometer. The anaerobic condition: a nitrogen-oxygen mixed gas with different oxygen content was injected into the solution for 30min, and the other conditions were consistent with normal oxygen conditions.

1.5 ROS production for NH₂-TPA (NO₂-TPA was activated by nitroreductase) in the presence and absence of oxygen in solution

NO₂-TPA (10 μ M) and NTR (1.67 μ g/mL) and NAD⁺ (66.7 μ M) were dissolved in 3 mL double purified water and incubated at 37 °C for 5 min. DCFH (40 μ M) was then added to the quartz cuvette containing the above samples and illuminated by a xenon lamp of 5 mW cm⁻². The change of fluorescence intensity at 523 nm was recorded using a fluorescence spectrophotometer. The anaerobic condition: a nitrogen-oxygen mixed gas with different oxygen content was injected into the solution for 30 min, and the other conditions were consistent with normal oxygen conditions.

1.6 O₂⁻ production in the presence and absence of oxygen in solution

Because the wavelength of the photosensitive dye collides with the Superoxide anion fluorescence detection probe DHE, Dihydrorhodamine 123 (DHR123) was chosen as an alternative for the detection of superoxide anion in solution. The non-fluorescent substance DHR123 can be oxidized by O₂⁻ and produces fluorescence at 525 nm. **NO₂-TPA** (10 μ M) and DHR123 (40 μ M) were dissolved in 3 mL double purified water. The mixture was placed in a quartz cuvette and illuminated by a xenon lamp of 5 mW cm⁻². The change of fluorescence intensity at 525 nm was recorded using a fluorescence spectrophotometer. The anaerobic condition was evaluated by injection with a nitrogen-oxygen mixed gas with different oxygen content for 30 min, and the other conditions were consistent with normal oxygen conditions.

1.7 O₂⁻ production for NH₂-TPA (NO₂-TPA was activated by nitroreductase) in the presence and absence of oxygen in solution

NO₂-TPA (10 μM) and NTR (1.67 μg/mL) and NAD⁺ (66.7 μM) were dissolved in 3 mL double purified water and incubated at 37 °C for 5 min. DHR123 (40 μM) was then added to the quartz cuvette containing the above samples and illuminated by a xenon lamp of 5 mW cm⁻². The change of fluorescence intensity at 525 nm was recorded using a fluorescence spectrophotometer. The anaerobic condition was evaluated by injection with a nitrogen-oxygen mixed gas with different oxygen content for 30 min, and the other conditions were consistent with normal oxygen conditions.

1.8 EPR evaluation of probes NO₂-TPA, NH₂-TPA and H-TPA

Superoxide free radical capture: The probe NO₂-TPA, NH₂-TPA and H-TPA (10 μM) were dissolved into methanol solution respectively, and the trapping agent DMPO (100 mM) was added. Anoxic conditions were achieved by ventilating with nitrogen for 30min to purge oxygen. The illumination is carried out by 396 nm xenon lamp (12.5 mW cm⁻²).

Persistent free radical capture: Powder samples were evaluated directly in the quartz tube. Light conditions were obtained by irradiation using a xenon lamp, dark conditions with no light irradiation. Test conditions: center field 3420 G, scanning range 100 G, microwave frequency: 9.60 GHz, power: 3.162 mw, amplitude: 1 G, time constant: 1.28 ms, conversion time: 25 ms, receiving gain: 40 dB, scanning time: 25 s.

1.9 Cell culture

HepG-2 cell lines and HL-7702 cell lines were obtained from the Chinese Academy of Medical Sciences. The red-free Dulbecco's Modified Eagle's Medium (DMEM, WelGene) supplemented with 1 % penicillin/streptomycin and 10% fetal bovine serum (FBS; Gibco) was used to culture cells in a CO₂ incubator at 37 °C.

1.10 Cell viability assay

HL-7702 and HepG-2 were selected as research objects for experimental testing. The two kinds of cells were inoculated in 96-well plates (5×10³ cells well⁻¹) respectively, and then placed in an incubator with 5 wt%/vol CO₂ at 37 °C for 24 h to make the cells stick to the wall. The cells were incubated for an additional 24 h with NO₂-TPA, NH₂-TPA and H-TPA at different concentrations. In the light group test, cell phototoxicity irradiator (Puri Material Technology Co., LTD.) was used to irradiate for 20 min (12.5 mW cm⁻², 396 nm), 1h after the probe was

added. Subsequently, 20 μL of 3-(4,5-dimethylthiazol-2-yl)-2,5-diphenyltetrazolium bromide (MTT, Sigma Chemical Co. U.S.A.) was added into each well, followed by further incubation for 4 h at 37°C. Finally, DMSO was added at 150 μL to the well after pouring out all the liquid in the 96-well plate. The absorbance OD value at 490 nm was measured by enzyme-labeled meter (Spectra Max M5, Molecular Devices). The experimental data were obtained by averaging the data of three parallel experiments.

1.11 ROS production in cells

HepG-2 cells were inoculated in confocal culture dishes for 16 h and then cultured under conditions of 2 % O_2 , 1 % O_2 and < 0.01 % O_2 for 8 h. **NO_2 -TPA** (6 μM) or **NH_2 -TPA** (6 μM) was added into the culture dish for 40 min, then washed with PBS. After adding DCFH (6 μM) to culture for 20 min, washed with PBS before adding 2 mL DMEM medium. The petri dishes were irradiated by xenon lamp (12.5 mW cm^{-2}) for 3 min, and the fluorescence signal of DCF in cells was captured by Olympus FV1200 laser confocal microscope.

1.12 O_2^- production in cells

HepG-2 cells were inoculated in confocal culture dishes for 16 h and then cultured under conditions of 2 % O_2 , 1 % O_2 and < 0.01 % O_2 for 8 h. **NO_2 -TPA** (6 μM) or **NH_2 -TPA** (6 μM) was added into the culture dish for 40 min, then washed with PBS. After adding DHR123 (6 μM) to culture for 20 min, washed with PBS before adding 2 mL DMEM medium. The petri dishes were irradiated by xenon lamp (12.5 mW cm^{-2}) for 3 min, and the fluorescence signal of oxidized DHR123 in cells was captured by Olympus FV1200 laser confocal microscope.

1.13 HepG-2 mitochondrial membrane potential in PDT experiment

HepG-2 cells were inoculated in confocal culture dishes for 24 h. **NH_2 -TPA** was added and incubated for 40 min, then washed with PBS. The petri dishes were irradiated by xenon lamp (12.5 mW cm^{-2}) for different time (0, 5 and 20 min). Then JC-10 (10 μM) was added and cultured for 10 min. The fluorescence signal of oxidized JC-10 in cells was captured by an Olympus FV1200 laser confocal microscope.

1.14 In vivo imaging

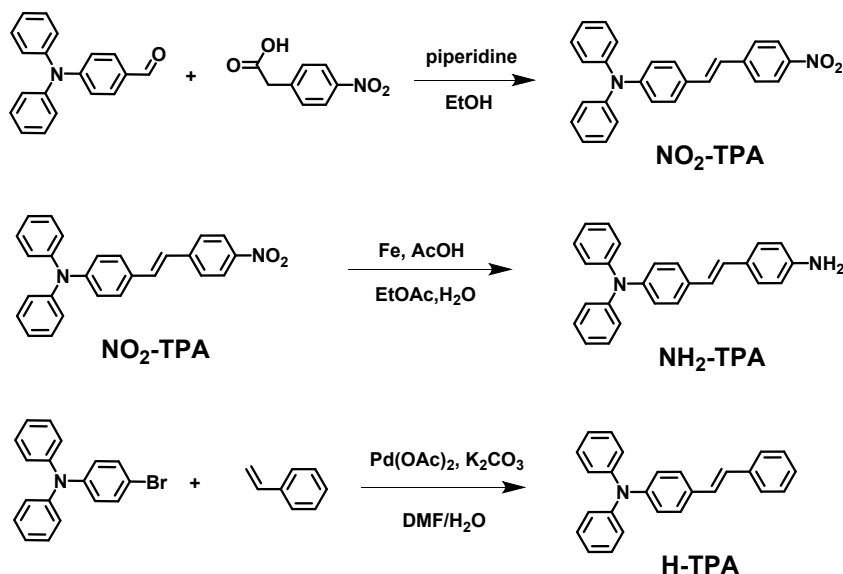
All animal experiments in this study were authorized by the local research ethics review board of the Xinxiang Medical University's Animal Ethics Committee (Henan, China, ethics statement Reference No. 2015016). Furthermore, all mice were employed in conformity with institutional ethics committee regulations and animal welfare recommendations.

Subcutaneous S180 implantation was used to establish a mouse tumor model in NU/NU nude mice. **NO₂-TPA** (1 mM, 10 μ L) was injected into tumor bearing mice, and then fluorescence imaging was performed on the small animal imaging instrument Night OWL II LB 983 to monitor the distribution of photosensitizer in the tumor.

1.15 PDT experiments

In order to verify the photosensitizers effective treatment effect on biological systems, Subcutaneous S180 implantation was used to establish a mouse tumor model in NU/NU nude mice and KM mice for PDT experiment. When the tumor volume reached 120 cm³, the mice were divided into 6 groups for treatment. Group 1: **NO₂-TPA** injection; Group 2: **NO₂-TPA** injection and light irradiation; Group 3: **NH₂-TPA** injection; Group 4: **NH₂-TPA** injection and light irradiation; Group 5: unprocessed; Group 6: light irradiation only. The method of injection was intratumoral injection. 30 min after injection, Group 2, Group 4 and Group 6 were irradiation by Xenon lamp irradiation (396 nm, 12.5 mW cm⁻²) treatment. The tumors were treated with injection and light at days 1,4,7,10 and 13. Efficacy was evaluated by measuring tumor volume and mouse weight at 22 days. The tumor was dissected 22 days later.

2. Synthesis of NO₂-TPA, NH₂-TPA and H-TPA



Scheme S1. Synthetic routes for NO₂-TPA, NH₂-TPA and H-TPA.

Synthesis of compound NO₂-TPA

A solution of 4-(diphenylamino) benzaldehyde (54.6 mg, 0.2 mmol) and 4-nitrophenyl acetic acid (54.3 mg, 0.3 mmol) was refluxed in dry ethanol catalyzed by a few drops of piperidine. The solvent was removed by rotary evaporation. The residue was purified using column chromatography using a petroleum ether and dichloromethane mixture (2: 1 v/v) as the eluting solvent to obtain **NO₂-TPA** as an orange red solid (40.3 mg, 51.5 % yield). ¹H NMR (600 MHz, CDCl₃) δ 8.20 (d, *J* = 8.6 Hz, 2H), 7.59 (d, *J* = 8.7 Hz, 2H), 7.42 (t, *J* = 9.6 Hz, 2H), 7.29 (t, *J* = 7.8 Hz, 4H), 7.21 (d, *J* = 16.3 Hz, 2H), 7.13 (d, *J* = 8.2 Hz, 4H), 7.07 (dd, *J* = 14.4, 7.8 Hz, 4H), 7.01 (d, *J* = 16.2 Hz, 2H). ¹³C NMR (151 MHz, CDCl₃) δ 148.57, 147.22, 146.39, 144.33, 132.88, 129.76, 129.41, 127.98, 126.50, 124.97, 124.18, 123.59, 122.71. Q-TOF-MS: calcd for C₂₆H₂₀N₂O₂: 392.1525; found: 392.1522.

Synthesis of compound NH₂-TPA

Iron powder (1.20 g, 2 mmol) and acetic acid (8 mL) were added to 26 mL water and heated to 90 °C for 0.5 h, then molecule **NO₂-TPA** (94.5 mg, 0.2mmol) in 14 mL ethyl acetate was poured into the mixed solution, which was stirred under reflux for 7 h. After reaction, the mixture was extracted and filtered, the filtrate was extracted three times with ethyl acetate, and the organic phase was collected. The solvent was removed under reduced pressure to gain the crude product, which was purified by column chromatography using a petroleum ether and dichloromethane

mixture (1: 1 v/v) as the eluting solvent to obtain **NH₂-TPA** as a yellow solid (27.8 mg, 38.5 % yield). ¹H NMR (400 MHz, DMSO-*d*₆) δ 7.42 (d, *J* = 8.6 Hz, 2H), 7.34-7.27 (m, 4H), 7.24 (d, *J* = 8.5 Hz, 2H), 7.07-6.99 (m, 6H), 6.95 (d, *J* = 5.7 Hz, 1H), 6.92 (d, *J* = 2.0 Hz, 1H), 6.84 (d, *J* = 16.3 Hz, 1H), 6.55 (d, *J* = 8.5 Hz, 2H), 5.27 (s, 2H). ¹³C NMR (151 MHz, DMSO) δ 149.05, 148.47, 147.62, 146.09, 133.23, 129.99, 128.38, 127.91, 127.30, 126.10, 125.41, 124.21, 123.39, 122.73, 114.37. Q-TOF-MS: calcd for C₂₆H₂₃N₂⁺: 363.1861; found: 363.1868.

Synthesis of compound **H-TPA**

4-bromo-*N,N*-diphenylaniline (324 mg, 1 mmol), styrene (115 μL, 2 mmol), palladium acetate (22.5 mg, 0.1 mmol) and potassium carbonate (276 mg, 2 mmol) were added into 100 mL round-bottomed flask, and 10 mL of mixed solvent (DMF/H₂O = 4/1, v/v) was added and refluxed for 4 h. After the reaction was complete, the reaction liquid was cooled and filtered, to obtain a beige solid crude product. The crude product was purified by column chromatography with petroleum ether as eluent, to give **H-TPA** as an off-white solid (556 mg, 80 % yield). ¹H NMR (600 MHz, CDCl₃) δ 7.50 (d, *J* = 7.5 Hz, 1H), 7.40 (d, *J* = 8.6 Hz, 1H), 7.35 (t, *J* = 7.7 Hz, 1H), 7.28 (d, *J* = 7.6 Hz, 1H), 7.26-7.22 (m, 1H), 7.12 (d, *J* = 7.7 Hz, 1H), 7.09-7.02 (m, 1H), 7.01 (d, *J* = 16.3 Hz, 1H). ¹³C NMR (151 MHz, DMSO) δ 147.55, 147.36, 137.63, 131.52, 129.28, 128.65, 128.17, 127.35, 127.28, 127.05, 126.30, 124.48, 123.60, 123.02.

3. Properties of photosensitizers

Table S1. Basic Photophysical Data of NO₂-TPA, NH₂-TPA and H-TPA. ^a

Compound	Processing method	$\lambda_{\text{ex/one photon}}^b$ (nm)	$\epsilon \times 10^4$ (M ⁻¹ cm ⁻¹)	$\lambda_{\text{em-flu}}^c$ (nm)	Φ_{flu} (%)	$\lambda_{\text{em-ph}}^d$ (nm)	τ^e (ns)
NO ₂ -TPA	NO ₂ -TPA	456	2.66	660	0.27	630	2.30
	NO ₂ -TPA+NTR	456	2.50	655	0.31	— ^f	3.43
	NO ₂ -TPA+NAD ⁺	460	2.31	656	0.26	— ^f	4.16
	NO ₂ -TPA+NTR+NAD ⁺	474	2.07	666	0.52	— ^f	4.61
NH ₂ -TPA	NH ₂ -TPA	379	3.15	429/444	2.71	446/476	0.89
	NH ₂ -TPA+NTR	400	2.12	430/449	1.76	— ^f	0.81
	NH ₂ -TPA+NAD ⁺	379	2.96	429/444	2.06	— ^f	0.62
H-TPA	H-TPA	378	4.15	421	23.1	453	0.41
	H-TPA+NAD ⁺	379	4.02	422	21.4	— ^f	0.22

^a, All tests were carried out in H₂O, except that the phosphorescent emission was a solid test. ^b, Maximum absorption wavelength. ^c, Maximum fluorescence emission wavelength. ^d, Maximum phosphorescent emission wavelength. ^e, Fluorescence lifetime. ^f, No measurement.

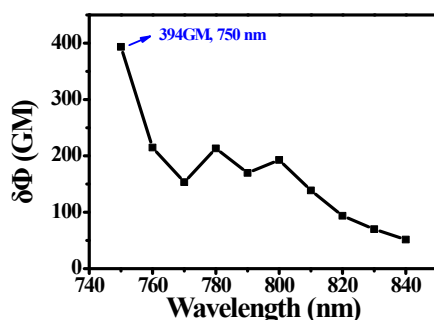


Figure S1. Two photon absorption spectrum of NO₂-TPA. (20 μ M in PBS, pH=7.4).

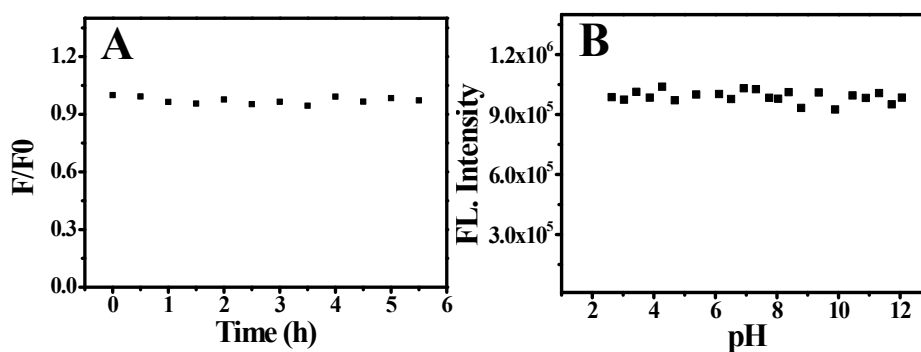


Figure S2. Stability of photosensitizer NO₂-TPA. (A) Changes in fluorescence intensity of photosensitizer NO₂-TPA under different time of illumination conditions (Iodine tungsten lamp, white light, 500W). (B) Fluorescence intensity of photosensitizer NO₂-TPA in different pH solutions.

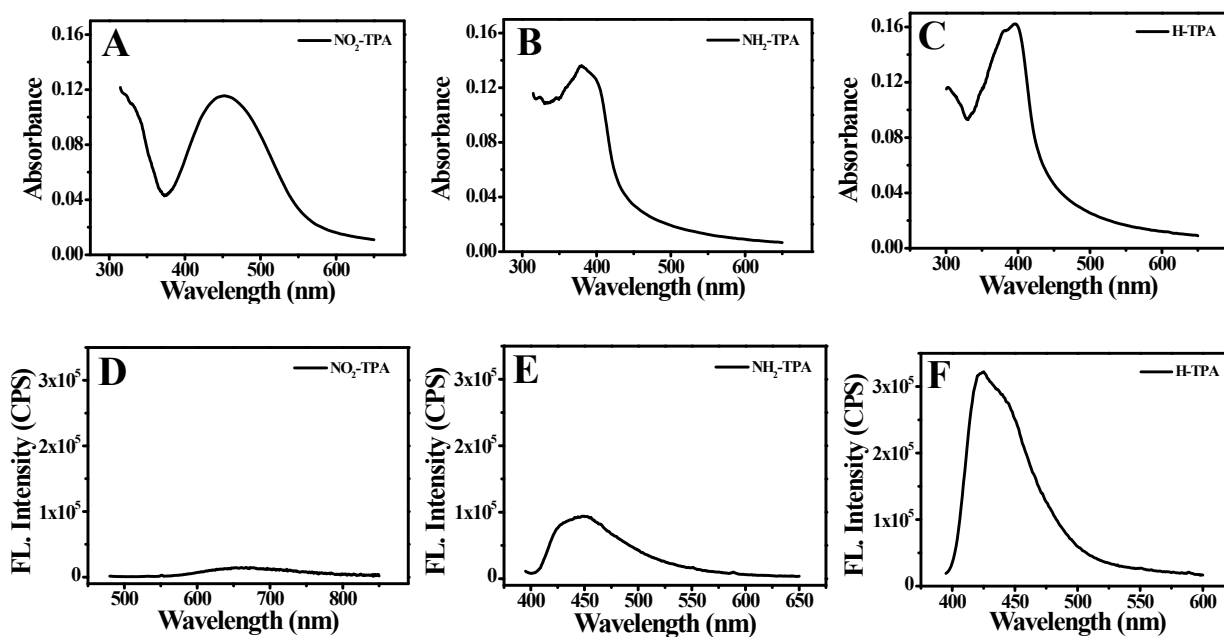


Figure S3. (A-C) Absorption spectra of NO₂-TPA, NH₂-TPA and H-TPA in aqueous solution; (D-F) Fluorescence spectra of NO₂-TPA, NH₂-TPA and H-TPA in aqueous solution. (Test concentration: 6 μM)

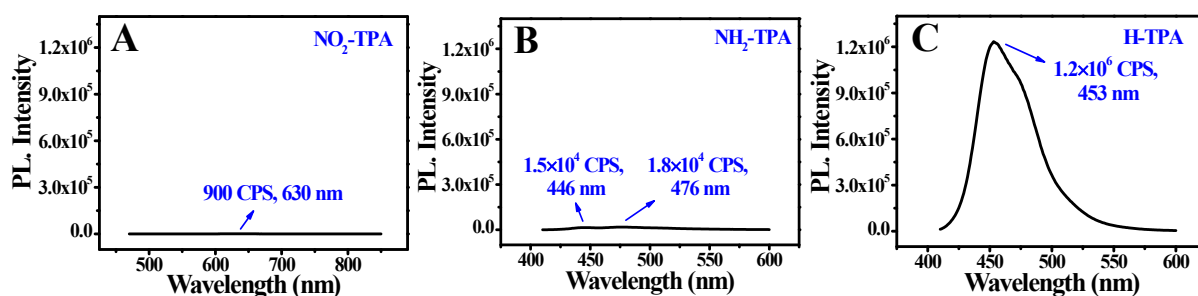


Figure S4. Phosphorescence spectra of (A) NO₂-TPA, (B) NH₂-TPA and (C) H-TPA in aqueous solution. (Solid test, Edinburgh FLS1000)

Table S2. Theoretical calculation data for **NO₂-TPA**, **NH₂-TPA** and **H-TPA**.

Compound	NO ₂ -TPA	NH ₂ -TPA	H-TPA
S ₁ (eV)	2.43	3.04	2.98
T ₁ (eV)	1.48	1.49	2.24
T ₂ (eV)	2.95	3.30	4.54
T ₃ (eV)	3.18	3.49	5.16
T ₄ (eV)	3.20	3.57	5.44
T ₅ (eV)	3.45	3.75	5.45
S ₁ -T ₁ (cm ⁻¹)	0.63	0.29	0.67
S ₁ -T ₂ (cm ⁻¹)	0.30	0.04	0.095
S ₁ -T ₃ (cm ⁻¹)	0.02	0.66	0.84
S ₁ -T ₄ (cm ⁻¹)	1.52	0.50	0.60
K _{isc} (S ₁ -T ₁) (S ⁻¹)	1.58×10 ⁴	1.12×10 ³	1.07×10 ⁵
K _{risc} (S ₁ -T ₁) (S ⁻¹)	3.98×10 ³	8.27×10 ²	9.48×10 ¹

In order to characterize ROS production in real time, a convenient fluorescence method was used for the detection of O₂-Type process. When DCFH (Figure S5A) was present in the test system, a clear fluorescence enhancement signal was observed for NH₂-TPA. But, no specific signal for singlet oxygen (¹O₂) was detected when 9,10-anthracenediyl-bis(methylene)-dimalonic acid (ABDA, a specific tracer agent for ¹O₂, Figure S5D) is present in the test system.

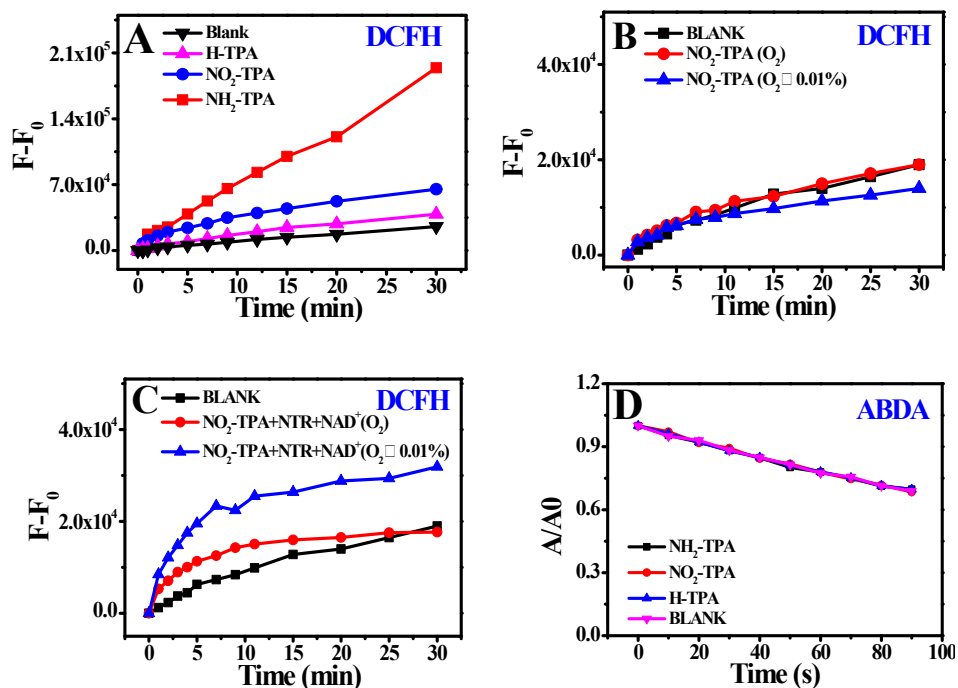


Figure S5. (A) Relative changes in fluorescence intensity of DCFH (40 μM) in the presence of NH₂-TPA, NO₂-TPA, H-TPA that was irradiated by light for different times. (B) Relative changes in fluorescent intensity of DCFH (40 μM) an indicator for various types of reactive oxygen species (ROS), were measured when NO₂-TPA (10 μM) was exposed to light irradiation for different durations in the presence or absence of oxygen. (C) Relative changes in fluorescence intensity of DCFH (40 μM) in the presence of NO₂-TPA (10 μM), NTR and NAD⁺ irradiated with or without oxygen. (D) ABDA (40 μM, for ¹O₂ detection) degradation induced by NH₂-TPA (10 μM), NO₂-TPA (10 μM) and H-TPA (10 μM) under light irradiation.

ROS fluorescent indicator was selected to test the production of $\text{NO}_2\text{-TPA}$ reactive oxygen species in the presence of a large amount of NAD^+ . The results indicated that no obvious signal enhancement was detected by DCFH after $\text{NO}_2\text{-TPA}$ molecules were illuminated in the presence of NAD^+ , indicating that there was no ROS production.

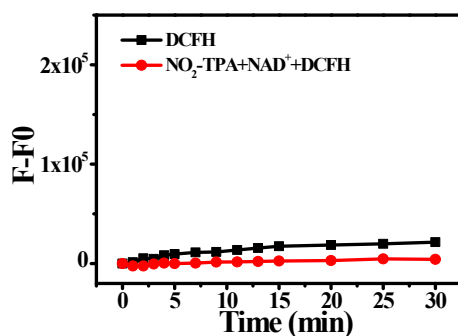


Figure S6. Relative changes in fluorescence intensity of DCFH (40 μM , ROS detection) for $\text{NO}_2\text{-TPA}$ and NAD^+ upon light irradiation for different times.

Free radical capture tests were performed on $\text{NO}_2\text{-TPA}$, $\text{NH}_2\text{-TPA}$ and H-TPA using EPR. The result of trapping agent DMPO on $\cdot\text{OH}$ was tested in aqueous solution. (Figure S7A) The capture results of $^1\text{O}_2$ with the capture agent TEMP were tested in methanol solution. (Figure S7B) The generation of nitrogen radicals was further verified by the detection of the photogenerated electron hole ability of $\text{NH}_2\text{-TPA}$ by EPR.

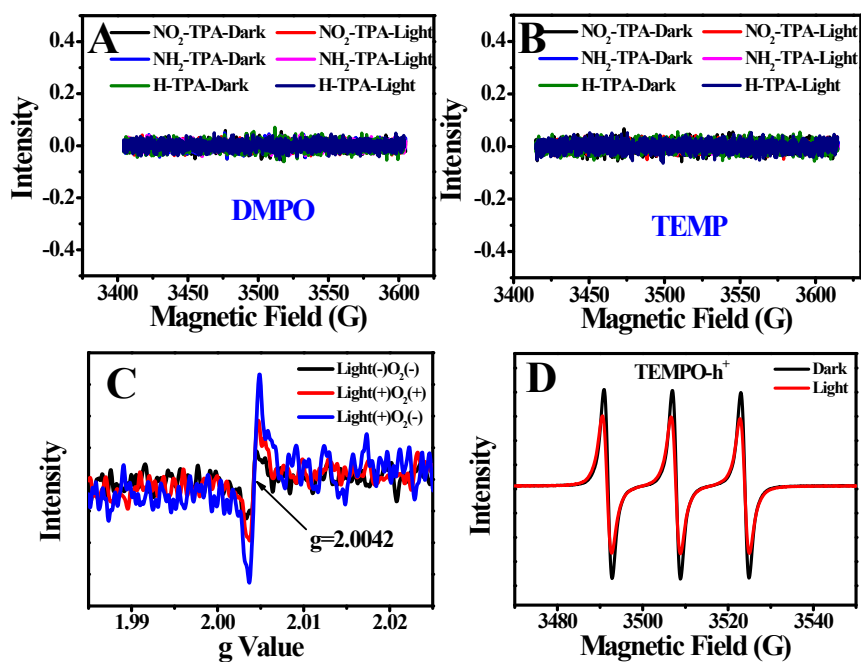


Figure S7. EPR spectrum detects $\cdot\text{OH}$ (A, solution: water) and $^1\text{O}_2$ (B, solution: methanol) of $\text{NO}_2\text{-TPA}$, $\text{NH}_2\text{-TPA}$, and H-TPA with or without light irradiation. (C) EPR spectra, nitrogen radical of $\text{NH}_2\text{-TPA}$ under normal or hypoxia with or without light. Light (+): with light irradiation; Light (-): without light irradiation; O_2 (+): normoxia; O_2 (-): hypoxia. (D) Photogenerated electron-hole signals of $\text{NH}_2\text{-TPA}$. (Capture agent: TEMPO; solution: methanol).

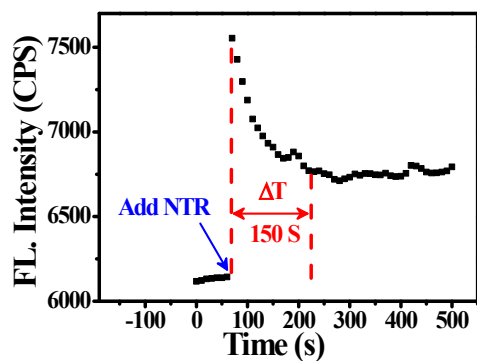


Figure S8. Time response relationship between NO₂-TPA and NTR.

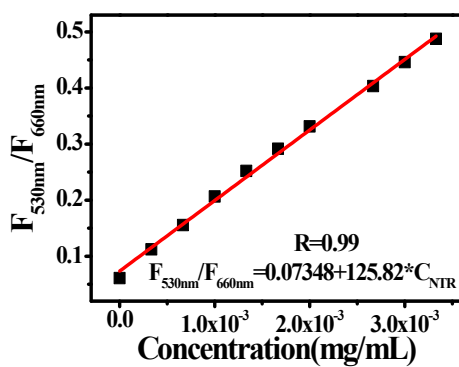


Figure S9. Linear relationship for the intensity ratio between NO₂-TPA and NTR response at 530 nm and 660 nm.

4. Establishing an anoxic model in solution

A nitrogen-oxygen mixed gas with different concentrations of oxygen was injected into the solution, and then the fluorescence signal was detected using an oxygen indicating probe (4,7-diphenyl-1,10-phenanthroline) ruthenium (II) dichloride ($[\text{Ru}(\text{dpp})_3\text{Cl}_2]$). The relationship between oxygen content and fluorescence intensity was plotted and shown in Figure S10. A model for solution anoxia of different degrees was established: nitrogen was injected into the solution at different times to eliminate oxygen to establish an anoxic test solution. Then anoxic probe ($[\text{Ru}(\text{dpp})_3\text{Cl}_2]$) was used to measure the fluorescence intensity of the test solution, and the intensity was substituted into the equation of oxygen content - fluorescence intensity to calculate the oxygen content in the solution.

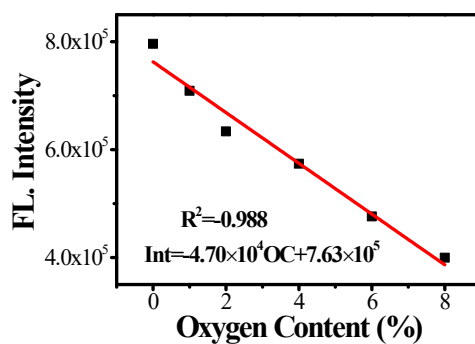


Figure S10. Oxygen content regression equation.

5. Transient absorption spectra and electron receptor quenching evaluation

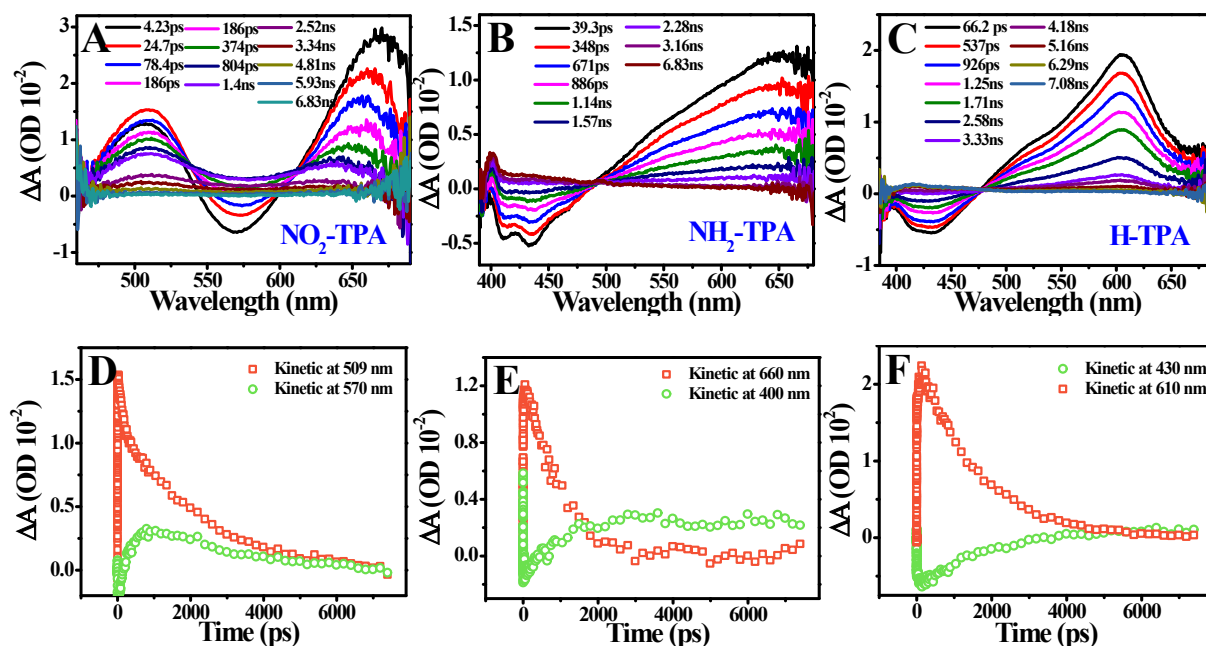


Figure S11. Femtosecond transient absorption spectra of $\text{NO}_2\text{-TPA}$ (A); $\text{NH}_2\text{-TPA}$ (B) and H-TPA (C) in methylbenzene at room temperature. The kinetic decay trajectories of $\text{NO}_2\text{-TPA}$ (D); $\text{NH}_2\text{-TPA}$ (E) and H-TPA (F) at different wavelengths were monitored.

6. TCNQ induces electron transfer

Fluorescence quenching experiments of $\text{NO}_2\text{-TPA}$ and $\text{NH}_2\text{-TPA}$ were carried out using electron acceptor TCNQ. The results show that TCNQ can undergo obvious electron transfer with $\text{NH}_2\text{-TPA}$ in the excited state, quenching the fluorescence signal, but has no effect on the fluorescence signal of $\text{NO}_2\text{-TPA}$.

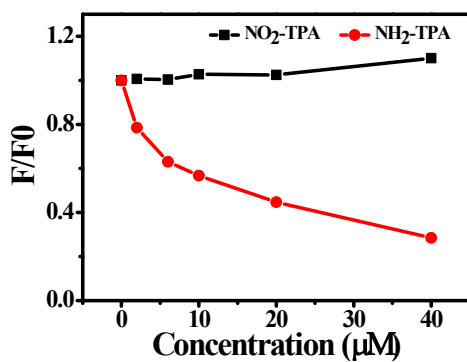


Figure S12. Changes in fluorescence intensity of $\text{NO}_2\text{-TPA}$ (black line) and $\text{NH}_2\text{-TPA}$ (red line) induced by TCNQ (40 μM).

7. Excited S1 state REDOX potential

The REDOX potential of **NO₂-TPA**, **NH₂-TPA** and **H-TPA** was measured by cyclic voltammetry. Three electrode organic system was used in the experiment. The measurement was performed in a dry and anaerobic acetonitrile solution containing 0.1 M tetrabutylammonium hexafluorophosphate (as a supporting electrolyte). A glass carbon electrode was selected as working electrode, Ag/Ag⁺ electrode was used as reference electrode, and Pt electrode as the opposite electrode. Fc/Fc⁺ was used as the internal parameter and the scan rate was 50 mV/s. The REDOX potential of S1 excited state was calculated according to the following equation (1).

$$E^*_{OX(compound)} = E_{OX(compound)} - E_{S1(compound)} \dots \dots \dots (1)$$

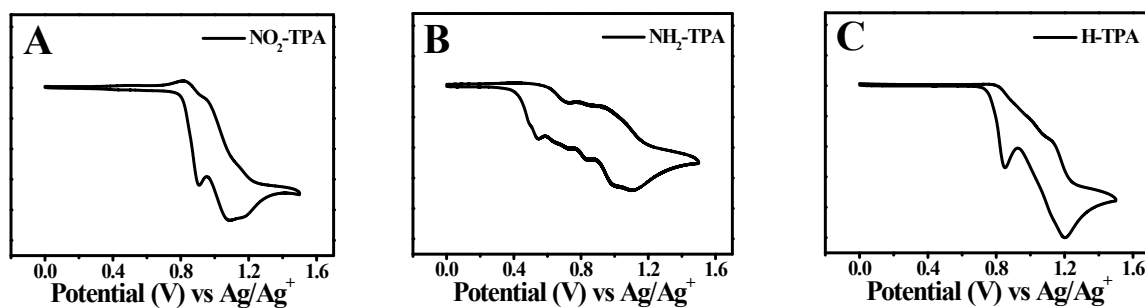


Figure S13. Cyclic voltammograms of **NO₂-TPA**, **NH₂-TPA** and **H-TPA** in acetonitrile with 0.1 M (n-Bu)₄N⁺PF₆⁻ as supporting electrolyte, glassy carbon electrode as a working electrode, Ag/Ag⁺ as a reference electrode, Pt electrode as a counter electrode. Fc/Fc⁺ was used as internal reference (scan rate = 50 mV/s).

Table S3. Oxidation potential of **NO₂-TPA**, **NH₂-TPA** and **H-TPA**.

Compound	Oxidation potential (V, vs Ag/Ag ⁺)	Oxidation potential (V, vs SCE)	Energy level (S1)	Excited state oxidation potential (V)
NO₂-TPA	0.90	0.81	2.43	-1.58
NH₂-TPA	0.53	0.44	3.04	-2.60
H-TPA	0.85	0.76	2.98	-2.22

8. Lipid droplet colocalization experiments

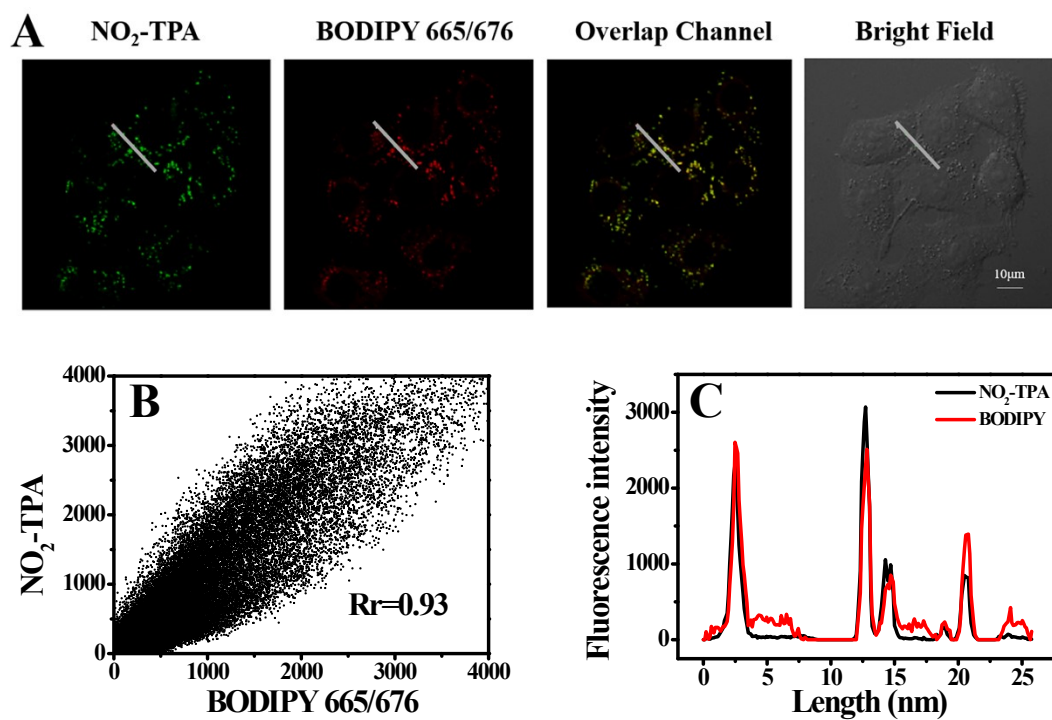


Figure S14. (A) Colocalization imaging experiments of NO₂-TPA (9 µM, Ex: 405 nm, Green Channel: 500-550 nm) with lipid drop commercial dye BODIPY 665/676 (9 µM, Ex: 635 nm, Red Channel: 660-720 nm). Scale bars: 10 µm. (B) Scatter plot of colocalization intensity correlation. (C) Linear correlation plot of colocalization intensity.

9. MTT Cell survival assay

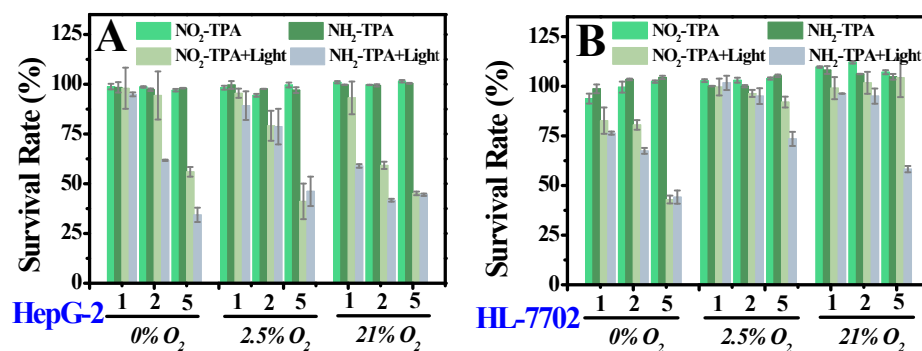
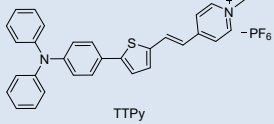
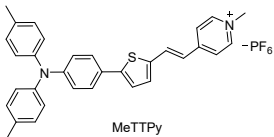
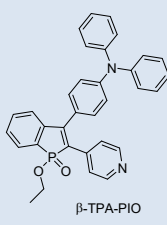
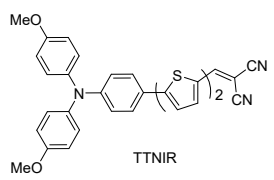
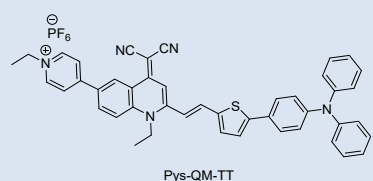
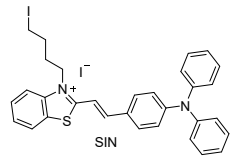
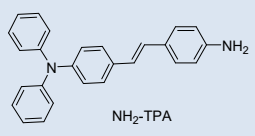
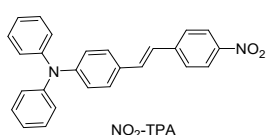


Figure S15. (A) Phototoxicity and dark toxicity of NO₂-TPA and NH₂-TPA to HepG-2 cells at different oxygen concentrations. (B) Phototoxicity and dark toxicity of NO₂-TPA and NH₂-TPA to HL-7702 cells at different oxygen concentrations. Test conditions: irradiation time: 20 min. Concentration: 1, 2 and 5 μM.

Table S4. Cellular phototoxicity of triphenylamine photosensitive dyes in the previous literature

The structure of photosensitive dyes	Cell survival under light conditions at a concentration of 5 μ M.	References
 <p>TTPy</p>	A431: 15% HLF: 65%	[1]
 <p>MeTTPy</p>	A431: 10% HLF: 50%	[1]
 <p>β-TPA-PIO</p>	Hela: 50%	[2]
 <p>TTNIR</p>	Hela: 30%	[3]
 <p>Pys-QM-TT</p>	Hela: <10%	[4]
 <p>SIN</p>	4T1: 50% MCF-7: 90% MDA-MB-231: 63%	[5]
 <p>NH₂-TPA</p>	HepG-2: 45% HL-7702: 60%	--
 <p>NO₂-TPA</p>	HepG-2: 46% HL-7702: 96%	--

10. Mitochondrial membrane potential laser confocal imaging

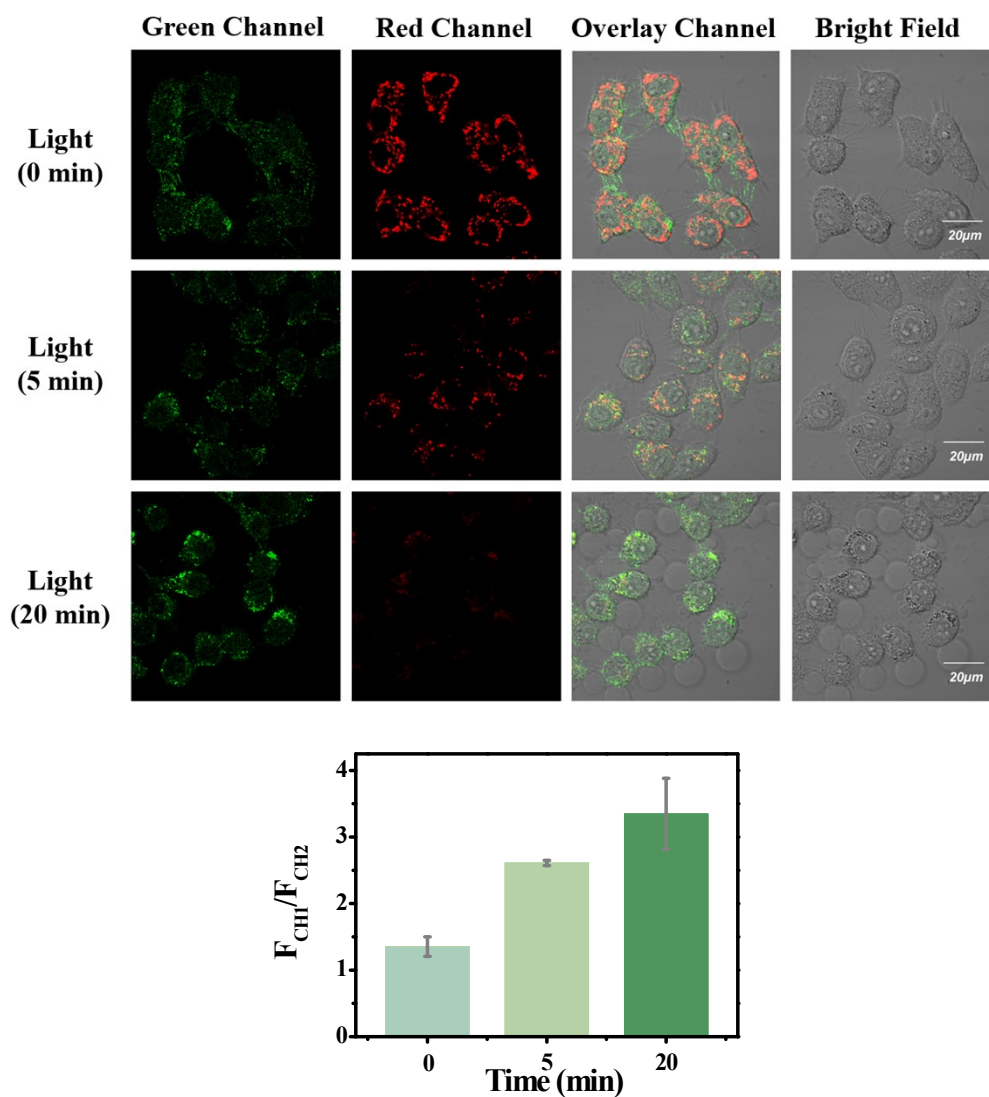


Figure S16. JC-10 (10 μ M) was used to monitor the changes of mitochondrial membrane potential in HepG-2 cells by NH₂-TPA under different illumination times. (Ex: 488 nm, 559 nm, Green Channel: 500-550 nm, Red Channel: 580 nm-620 nm).

11. High throughput cell flow cytometry

High throughput flow cytometry was used to detect the cell state after light treatment. According to the experimental results, the proportion of living cells was significantly reduced, and the proportion of dead cells was significantly increased in the HepG-2 cells treated with the photosensitive dye $\text{NO}_2\text{-TPA}$ and $\text{NH}_2\text{-TPA}$, indicating that the cells showed obvious programmed death after treatment with the photosensitive dye.

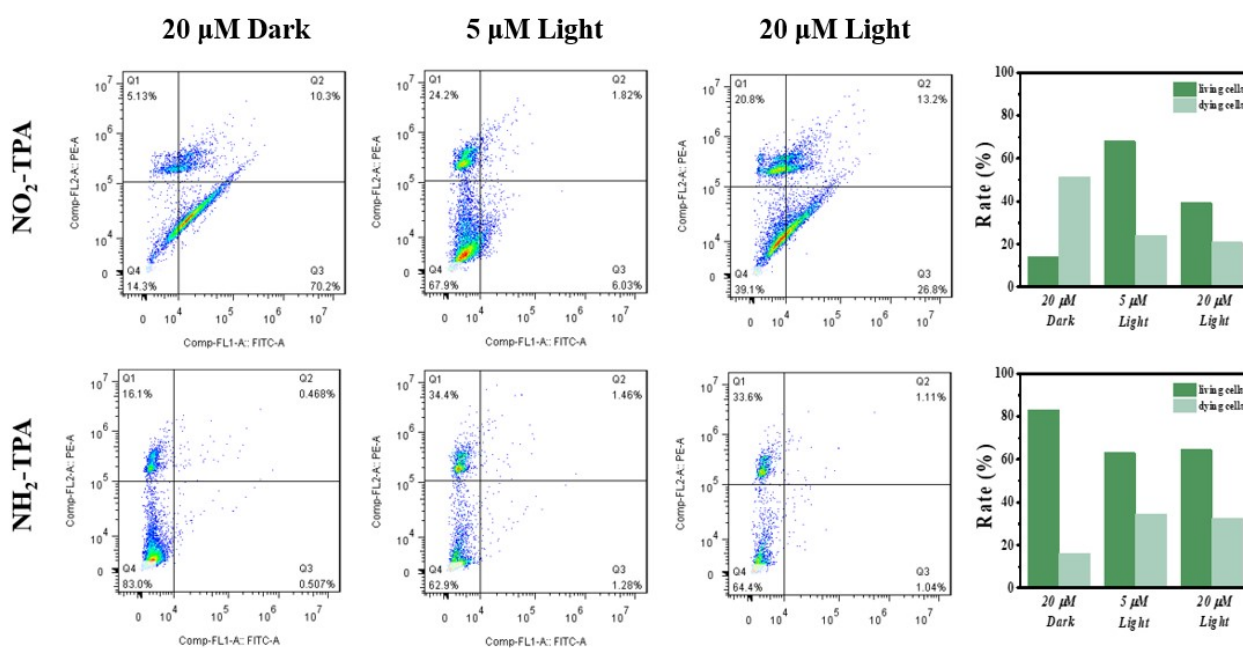


Figure S17. Flow cytometry of HepG-2 which were treated with $\text{NO}_2\text{-TPA}$ and $\text{NH}_2\text{-TPA}$ at different concentrations (5 μM and 20 μM) under dark conditions or with light irradiation.

12. Oxygen content in tumor tissue

In order to study the distribution of oxygen content in tumor tissue, we used sliced mouse tumor before and after treatment to prepare the tissue model, and then used commercial hypoxia probe ($[\text{Ru}(\text{dpp})_3]\text{Cl}_2$) to explore the oxygen content in tissue model.

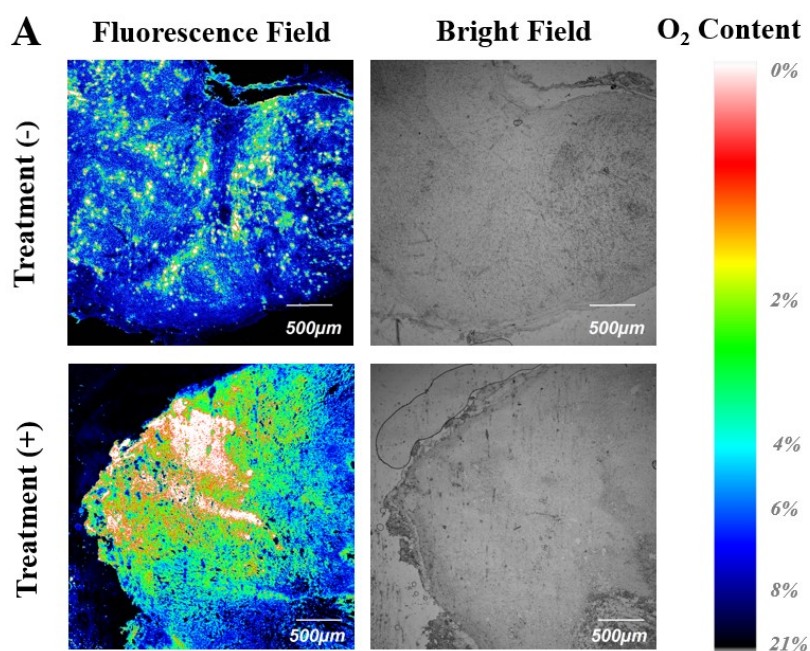


Figure S18. Laser confocal microscopic imaging of oxygen content in mouse tumor tissue. (Ex: 488 nm, Fluorescence Channel: 580 nm-640 nm, scale bars: 500 µm).

13. Fluorescence imaging of mouse tumors

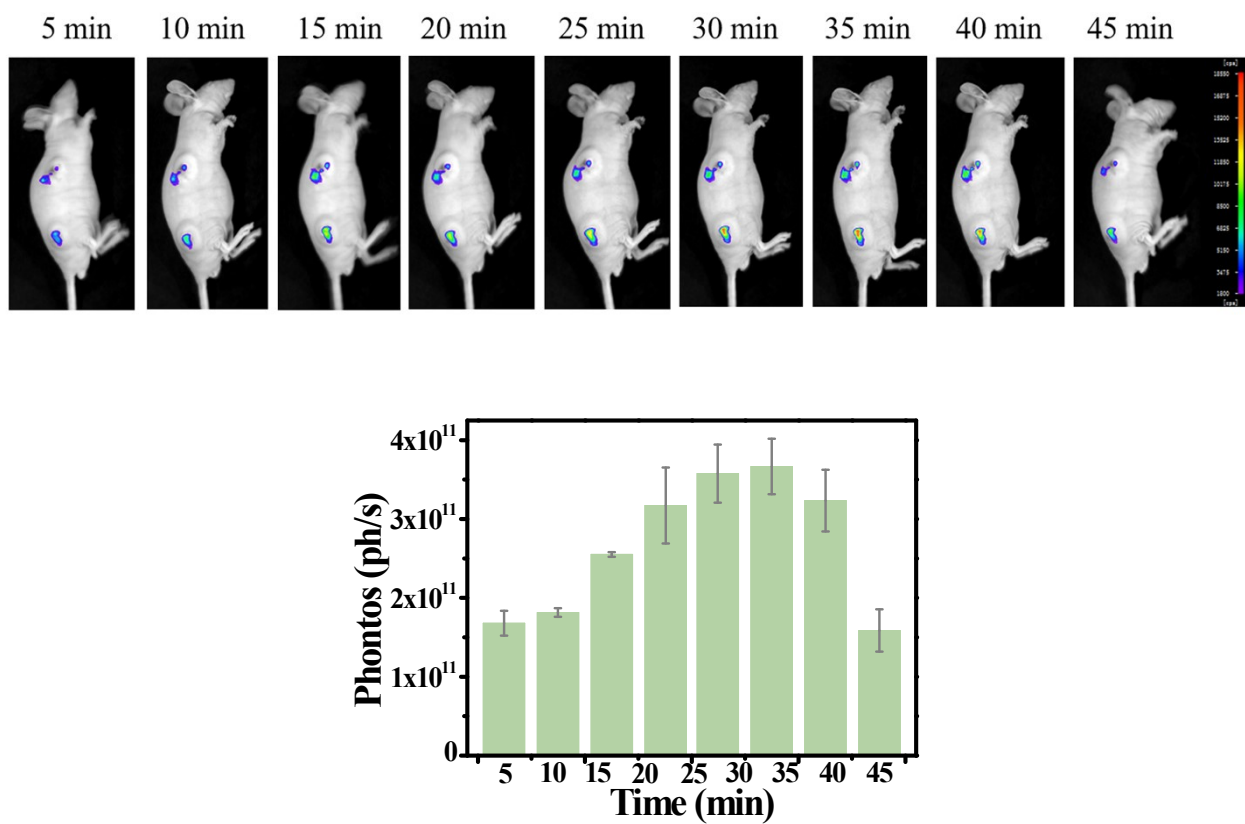


Figure S19. Fluorescence imaging of S180-tumor-bearing NU/NU nude mice over wavelength range from 530-570 nm by $\text{NO}_2\text{-TPA}$ at different times. The histogram shows tumor fluorescence intensity at different times.

14. NMR spectra and Q-TOF-MS

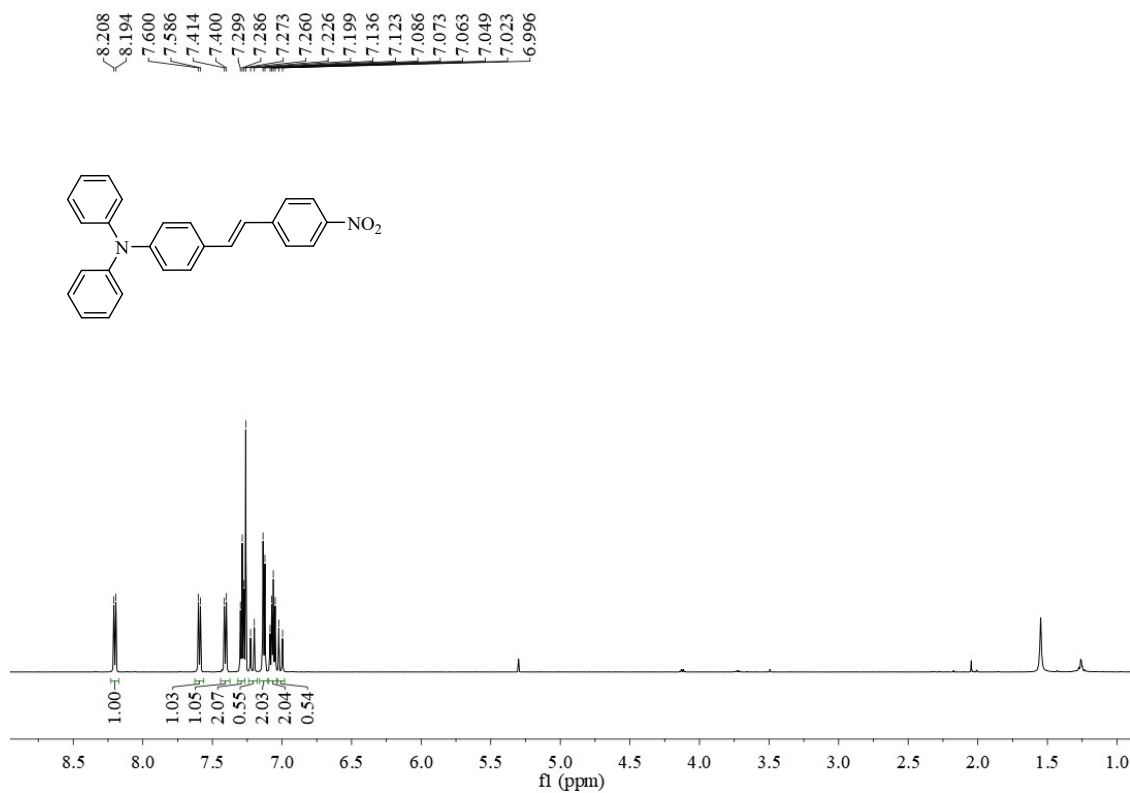


Figure S20. The ¹H NMR of NO₂-TPA

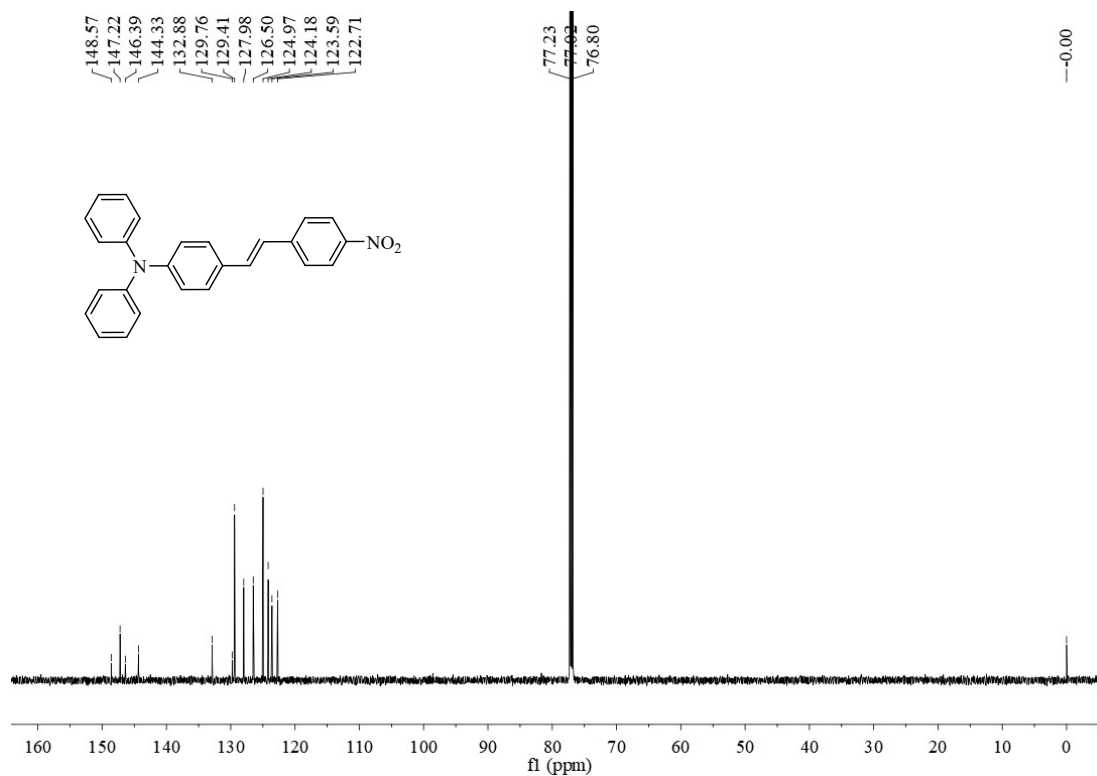


Figure S21. The ¹³C NMR of NO₂-TPA

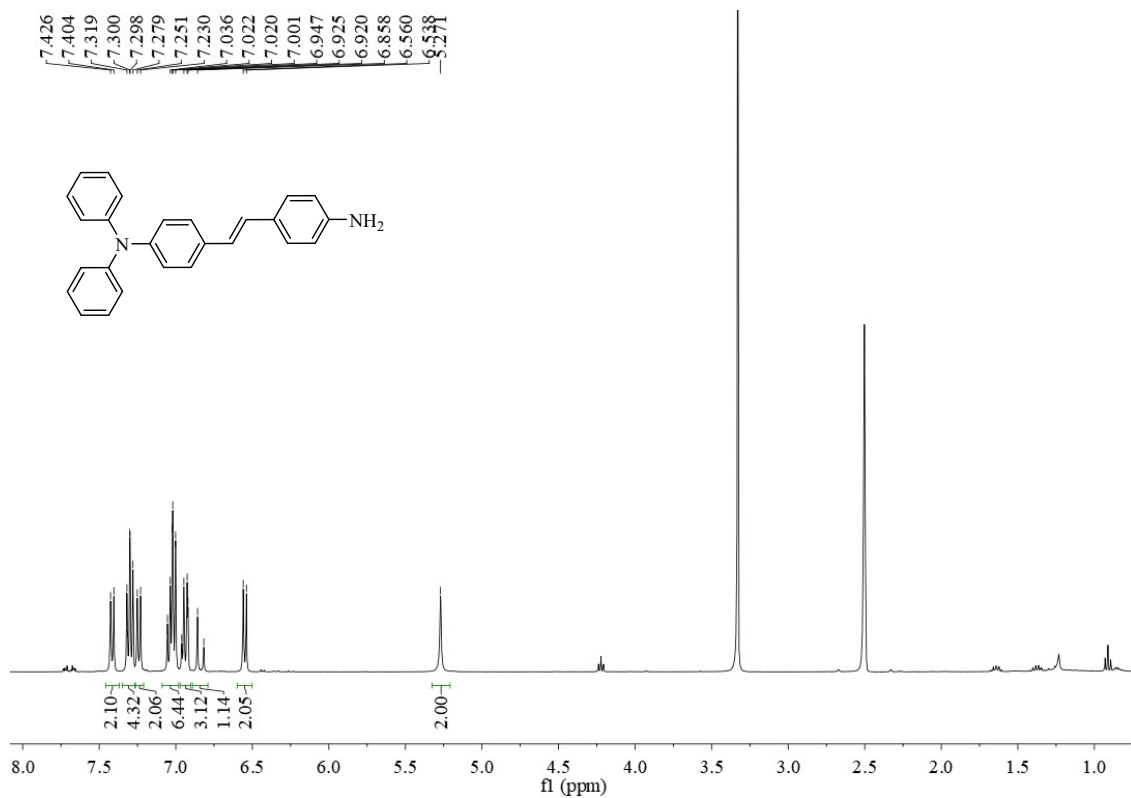


Figure S22. The ¹H NMR of NH₂-TPA

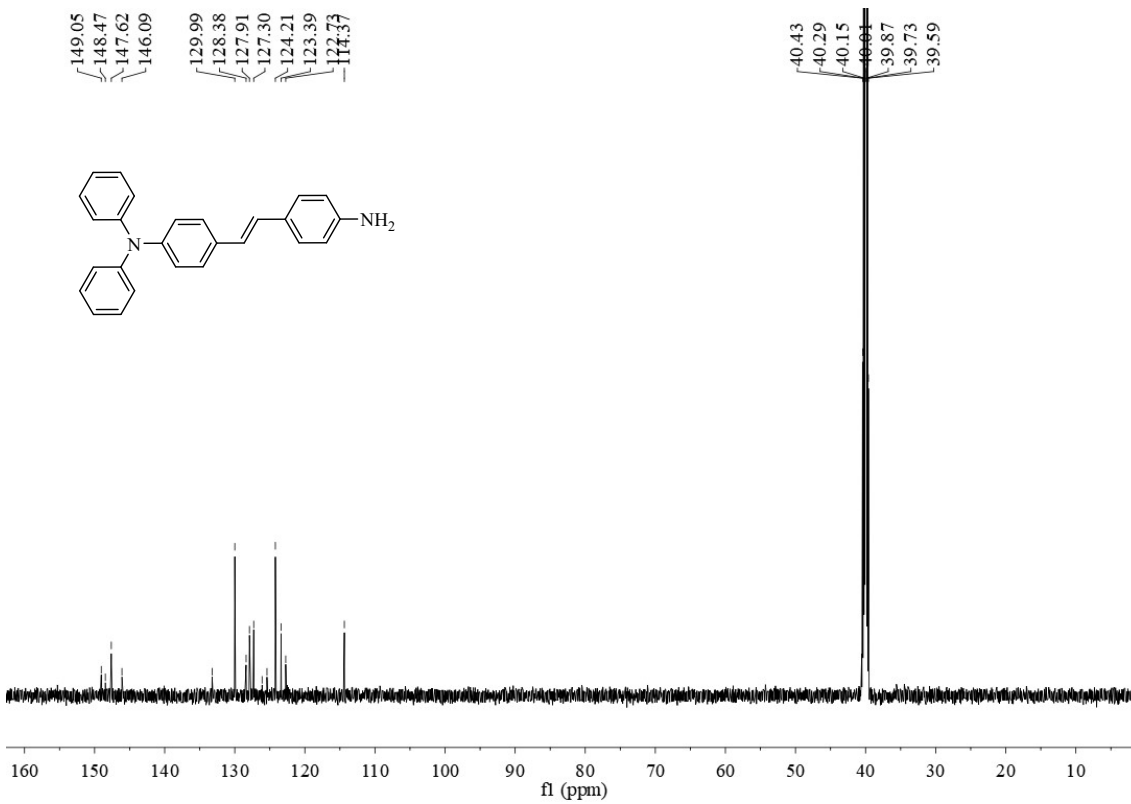


Figure S23. The ¹³C NMR of NH₂-TPA

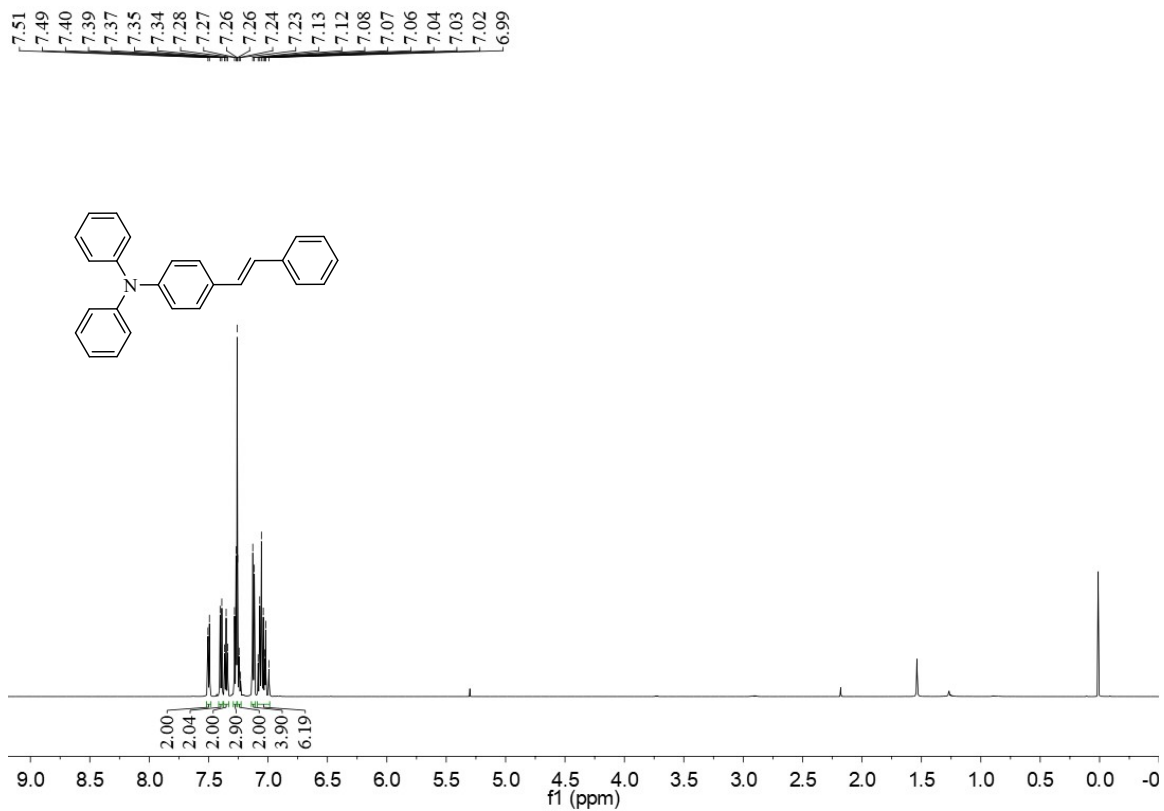


Figure S24. The ¹H NMR of H-TPA

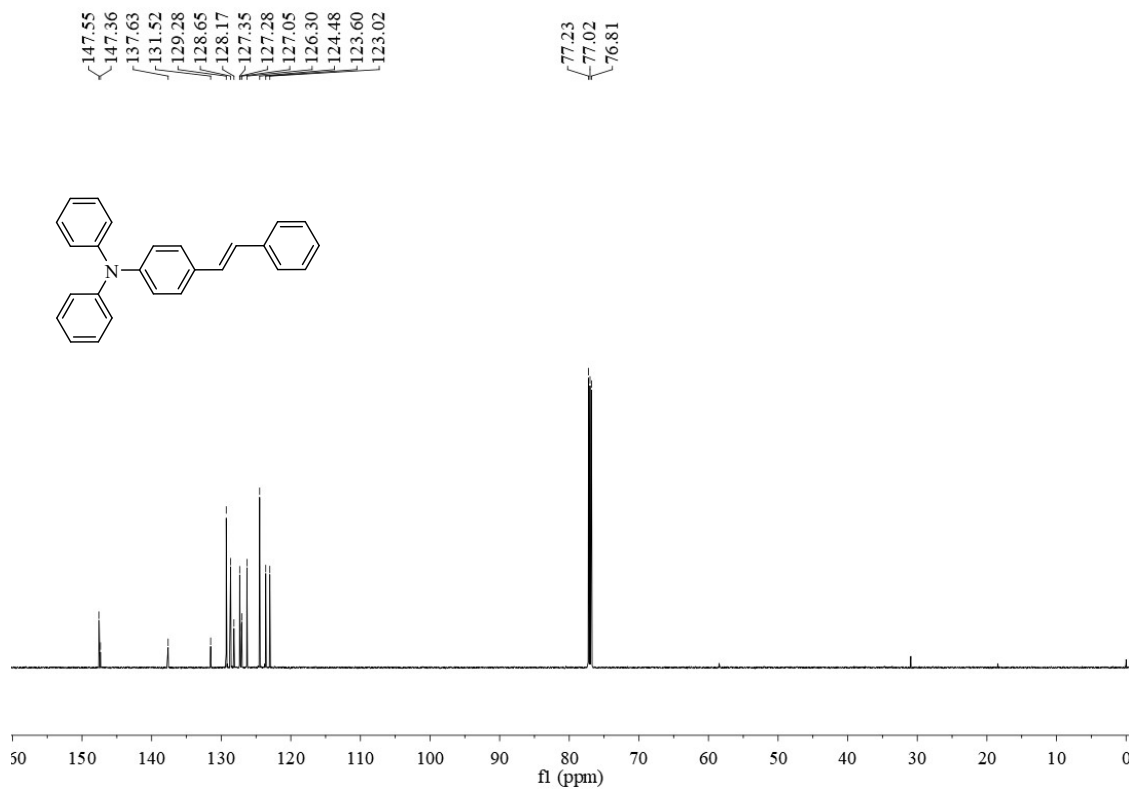


Figure S25. The ¹³C NMR of H-TPA

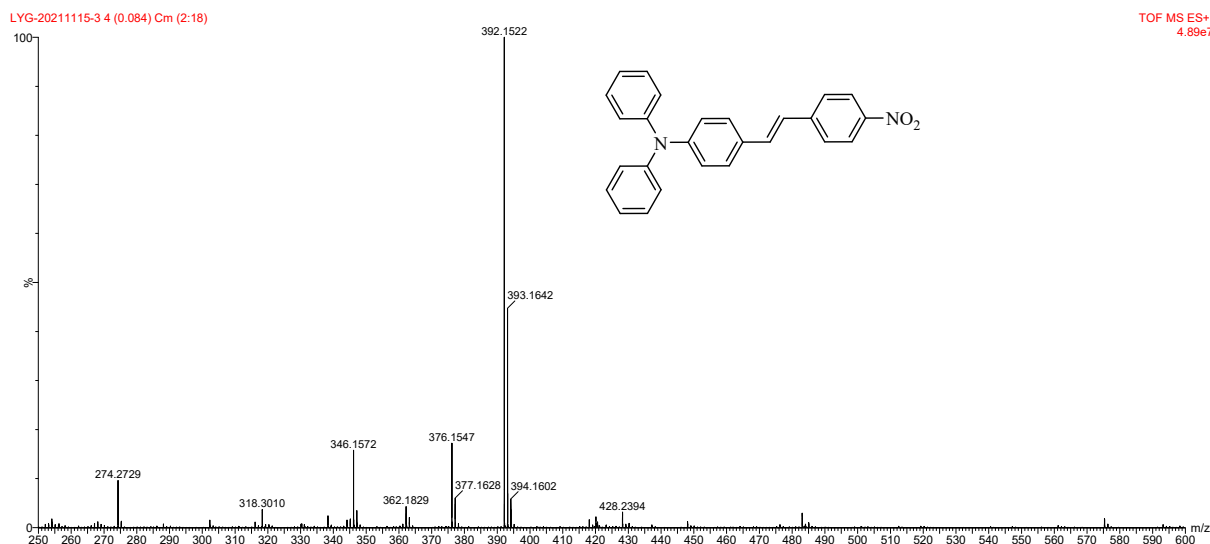


Figure S26. The Q-TOF-MS of NO₂-TPA

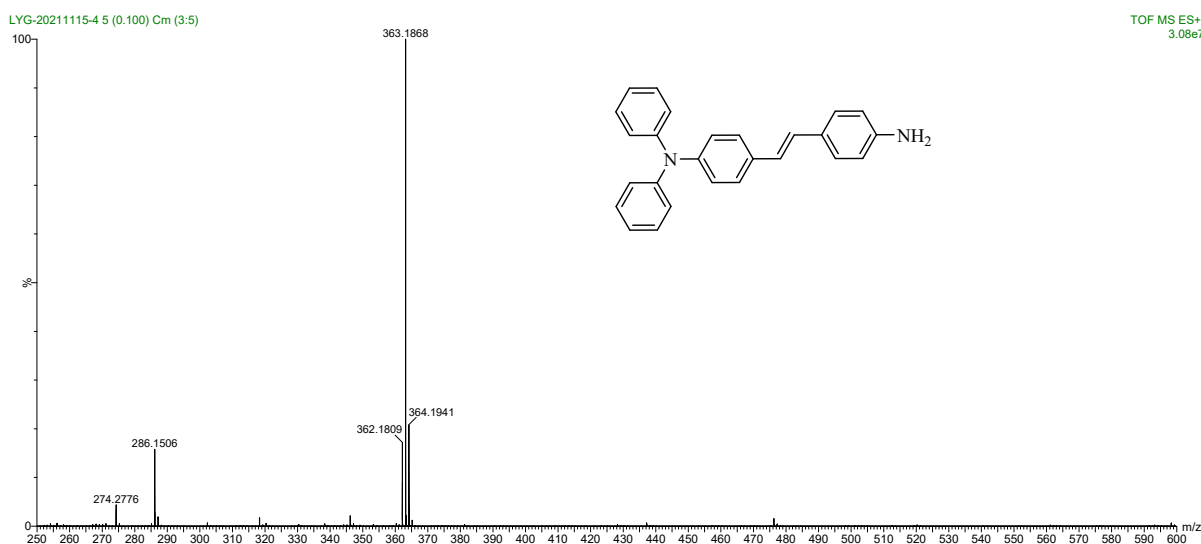


Figure S27. The Q-TOF-MS of NH₂-TPA

References

- [1] D. Wang, M. M. S. Lee, G. Shan, R. T. K. Kwok, J. W. Y. Lam, H. Su, Y. Cai and B. Z. Tang, *Adv. Mater.*, 2018, **30**, e1802105
- [2] Z. Zhuang, J. Dai, M. Yu, J. Li, P. Shen, R. Hu, X. Lou, Z. Zhao and B. Z. Tang, *Chem. Sci.* 2020, **11**, 3405-3417.
- [3] W. Xu, M. M. S. Lee, Z. Zhang, H. H. Y. Sung, I. D. Williams, R. T. K. Kwok, J. W. Y. Lam, D. Wang and B. Z. Tang, *Chem. Sci.* 2019, **10**, 3494-3501.
- [4] Y. Wang, J. Liao, Y. Lyu, Q. Guo, Z. Zhu, X. Wu, J. Yu, Q. Wang and W. H. Zhu, *Adv. Fun. Mater.* 2023, **33**, 2301692.
- [5] Z. Pan, Y. Wang, N. Chen, G. Cao, Y. Zeng, J. Dong, M. Liu, Z. Ye, Y. Li, S. Huang, Y.-j. Lu, Y. He, X. Liu and K. Zhang, *Bioorg. Chem.* 2023, **132**, 106349.